

## **Numerical methods for a quantum drift-diffusion equation in semiconductor physics**

**Ramón Escobedo and Luis L. Bonilla**

*Grupo de Modelización y Simulación Numérica,  
Escuela Politécnica Superior, Universidad Carlos III de Madrid,  
Av. de la Universidad 30, 28911 Leganés, Madrid – Spain.*

*emails: escobedo@math.uc3m.es, bonilla@ing.uc3m.es*

### **Abstract**

We present the numerical methods and simulations used to solve a charge transport problem in semiconductor physics. The problem is described by a Wigner-Poisson kinetic system we have recently proposed and whose results are in good agreement with known experiments. In this model we consider doped semiconductor superlattices in which electrons are supposed to occupy the lowest miniband, exchange of lateral momentum is ignored, the electron-electron interaction is treated in the Hartree approximation and elastic and inelastic collisions are taken into account. Nonlocal drift-diffusion equations derived systematically elsewhere from the hyperbolic limit of a kinetic Wigner-Poisson are solved. The non-locality of the original quantum kinetic model equations implies that the derived drift-diffusion equations contain spatial averages over one or more superlattice periods. Numerical methods are based upon prior knowledge on physical properties of the phenomenon and are shown to be effective enough in validating our formulation. Numerical solutions of the equations show self-sustained oscillations of the current through a voltage biased superlattice, in good agreement with known experiments.

*Key words: numerical methods, numerical simulations, nonlocal drift-diffusion equations, quantum kinetics*

*MSC 2000: 37M05, 37N20, 74S20, 81T80*

## 1 The model

Quantum kinetic descriptions of nonlinear charge transport in nanostructures give rise to difficult problems, which are costly to solve numerically [1]. Recently, a systematic way of deriving reduced balance equations for magnitudes such as the electron density or the local electric field which are cheaper to solve has been found for the case of the single-miniband Boltzmann-Poisson transport equation with a BGK (Bhatnagar-Gross-Krook [2]) collision term, for which drift-diffusion models of miniband transport in strongly coupled superlattices (SLs) have been deduced, obtaining a generalized drift-diffusion equation (GDDE) in the semiclassical limit [3, 4] and a quantum DDE (QDDE) in the case of quantum kinetics [5]. To solve these problems numerically, the prior knowledge of the physical phenomenon is crucial.

We present here the algorithm used to solve the QDDE, based on previous results obtained in the GDDE. In this model, we consider the Wigner equation for a strongly coupled SL with one miniband, we treat the electron-electron interaction in the Hartree approximation, we ignore exchange of momentum in the lateral directions and describe inelastic scattering within the BGK model [3, 4]. The resulting 1D model is sufficiently simple for a perturbative method to yield analytic expressions for the coefficients in the final QDDE. In contrast with the usual DDE's, the QDDE contains spatial averages of the electric field and other quantities and it is therefore *nonlocal* in space.

The Wigner-Poisson system for 1D electron transport in the lowest miniband of a strongly coupled SL is:

$$\begin{aligned} \frac{\partial f}{\partial t} + \frac{i}{\hbar} \left[ \mathcal{E}_1 \left( k + \frac{1}{2i} \frac{\partial}{\partial x} \right) - \mathcal{E}_1 \left( k - \frac{1}{2i} \frac{\partial}{\partial x} \right) \right] f \\ + \frac{ie}{\hbar} \left[ W \left( x + \frac{1}{2i} \frac{\partial}{\partial k}, t \right) - W \left( x - \frac{1}{2i} \frac{\partial}{\partial k}, t \right) \right] f \\ = -\nu_{\text{en}} (f - f^{FD}) - \nu_{\text{imp}} \frac{f(x, k, t) - f(x, -k, t)}{2}, \end{aligned} \quad (1)$$

$$\varepsilon \frac{\partial^2 W}{\partial x^2} = \frac{e}{l} (n - N_D), \quad (2)$$

$$n = \frac{l}{2\pi} \int_{-\pi/l}^{\pi/l} f(x, k, t) dk = \frac{l}{2\pi} \int_{-\pi/l}^{\pi/l} f^{FD}(k; n) dk, \quad (3)$$

$$\begin{aligned} f^{FD}(k; n) = \frac{m^* k_B T}{\pi^2 \hbar^2} \left\{ \tan^{-1} \left( \frac{\Gamma}{\mathcal{E}_1(k)} \right) \right. \\ \left. + \int_0^\infty \frac{\Gamma}{[E - \mathcal{E}_1(k)]^2 + \Gamma^2} \ln \left[ 1 + \exp \left( \frac{\mu - E}{k_B T} \right) \right] dE \right\}. \end{aligned} \quad (4)$$

Here  $f$ ,  $n$ ,  $N_D$ ,  $\mathcal{E}_1(k)$ ,  $d_B$ ,  $d_W$ ,  $l = d_B + d_W$ ,  $W$ ,  $\varepsilon$ ,  $m^*$ ,  $k_B$ ,  $T$ ,  $\Gamma$ ,  $\nu_{\text{en}}$ ,  $\nu_{\text{imp}}$

and  $-e < 0$  are the one-particle Wigner function, the 2D electron density, the 2D doping density, the miniband dispersion relation, the barrier width, the well width, the SL period, the electric potential, the SL permittivity, the effective mass of the electron, the Boltzmann constant, the lattice temperature, the energy broadening of the equilibrium distribution due to collisions, the frequency of the inelastic collisions responsible for energy relaxation, the frequency of the elastic impurity collisions and the electron charge, respectively. The chemical potential  $\mu$  is a function of  $n$  resulting from solving equation (3) with the integral of the collision-broadened 3D Fermi-Dirac distribution over the lateral components of the wave vector  $(k, k_y, k_z)$ , which is given by Eq. (4). Notice that, following Ignatov and Shashkin [9], we have not included the effects of the electric potential in our Fermi-Dirac distribution.

## 2 The Quantum Drift-Diffusion Equation

The derivation of the QDDE is explained in detail in Ref. [5]; here we only say that the procedure consists in deriving a form of Ampère's law for the current density from the hyperbolic limit of the Wigner equation, by means of a Chapman-Enskog ansatz. This leads to a linear hierarchy of equations with suitable solvability conditions, whose solution yields the first-order correction to the following Ampère's equation for the current density  $j(t)$ :

$$\varepsilon \frac{\partial F}{\partial t} + \frac{ev_M}{l} \langle n \mathcal{M} V(\mathcal{F}) \rangle_1 = j(t), \quad (5)$$

$$V(\mathcal{F}) = \frac{2\mathcal{F}}{1 + \mathcal{F}^2}, \quad F_M = \frac{\hbar}{el} \sqrt{\nu_e(\nu_{\text{en}} + \nu_{\text{imp}})}, \quad v_M = \frac{\Delta l \mathcal{I}_1(M)}{4\hbar\tau_e \mathcal{I}_0(M)}, \quad (6)$$

$$\mathcal{F} = \frac{\langle F \rangle_1}{F_M}, \quad \mathcal{M}(n/N_D) = \frac{\mathcal{I}_1(\tilde{\mu}) \mathcal{I}_0(M)}{\mathcal{I}_0(\tilde{\mu}) \mathcal{I}_1(M)}, \quad \mathcal{M}_2(n/N_D) = \frac{\mathcal{I}_2(\tilde{\mu}) \mathcal{I}_0(M)}{\mathcal{I}_0(\tilde{\mu}) \mathcal{I}_1(M)}, \quad (7)$$

$$\begin{aligned} \mathcal{I}_m(\tilde{\mu}) = & \frac{1}{\pi} \int_{-\pi}^{\pi} \cos(mk) \left[ \tan^{-1} \left( \frac{\tilde{\Gamma}/\delta}{1 - \cos k} \right) \right. \\ & \left. + \int_0^{\infty} \frac{\tilde{\Gamma}}{(\tilde{E} - \delta + \delta \cos k)^2 + \tilde{\Gamma}^2} \ln \left( 1 + e^{\tilde{\mu} - \tilde{E}} \right) d\tilde{E} \right] dk. \quad (8) \end{aligned}$$

Here  $F = -\partial W/\partial x$  is *minus* the electric field,  $v_M$  and  $F_M$  are the electron velocity and field scales,  $g'$  denotes  $dg/dn$ ,  $\delta = \Delta/(2k_B T)$ ,  $\Delta$  is the miniband width,  $\tilde{\mu} = \mu/(k_B T)$ ,  $\tau_e = \sqrt{(\nu_{\text{imp}} + \nu_{\text{en}})/\nu_{\text{en}}}$ ,  $\tilde{\Gamma} = \Gamma/(k_B T)$ , and  $n = N_D$  at the particular value of the dimensionless chemical potential  $\tilde{\mu} = M$ . We have used the average

$$\langle F \rangle_j(x, t) = \frac{1}{jl} \int_{-jl/2}^{jl/2} F(x + s, t) ds, \quad (9)$$

the tight-binding dispersion relation  $\mathcal{E}(k) = \Delta(1 - \cos kl)/2$ , and the usual miniband group velocity  $v(k) = (\Delta l/2\hbar)\sin kl$ . If the electric field and the electron density do not change appreciably over two SL periods,  $\langle F \rangle_j \approx F$ , the spatial averages can be ignored, and the *non-local* QDDE (5) becomes the *local* generalized DDE (GDDE) obtained from the semiclassical theory [3, 4].

Instead of reproducing here the *encumbering* first-order correction, we write the final QDDE in dimensionless form, which is much more suitable for numerical calculations:

$$\begin{aligned}
& E_t + \langle n\mathcal{M}V \rangle_1 + \kappa_1 \langle n\mathcal{M}G \langle \langle n\mathcal{M}V \rangle_1 \rangle_1 \rangle_1 \\
& - 4\kappa_2 \left\langle \frac{1}{1 + \mathcal{F}^2} \left( \left\langle \frac{n\mathcal{M}_2 \mathcal{F}_2 \langle E_x \rangle}{(1 + 4\mathcal{F}_2^2)^2} \right\rangle_1 + \frac{\mathcal{F}}{8} \left\langle \frac{n\mathcal{M}_2 (1 - 4\mathcal{F}_2^2) \langle E_x \rangle_2}{(1 + 4\mathcal{F}_2^2)^2} \right\rangle_1 \right) \right\rangle_1 \\
& + \kappa_3 \left\langle \frac{(n\mathcal{M})'V}{1 + \mathcal{F}^2} \left\langle \frac{n\mathcal{M} (1 - \mathcal{F}^2) \langle E_x \rangle_1}{(1 + \mathcal{F}^2)^2} \right\rangle_1 \right\rangle_1 = (1 + \kappa_1 \langle n\mathcal{M}G \rangle_1) J \quad (10) \\
& + \kappa_4 \left\langle \frac{1}{1 + \mathcal{F}^2} \langle E_{xx} \rangle_1 \right\rangle_1 - \frac{1}{2} \kappa_1 (1 + \tau_e^2) \left\langle \frac{(n\mathcal{M})'V}{1 + \mathcal{F}^2} \langle \langle (n\mathcal{M})'V E_{xx} \rangle_1 \rangle_1 \right\rangle_1 \\
& - \frac{1}{2} \kappa_2 \left\langle \frac{1}{1 + \mathcal{F}^2} \left\langle \frac{(n\mathcal{M}_2)'}{1 + 4\mathcal{F}_2^2} E_{xx} \right\rangle_1 \right\rangle_1 + \frac{1}{2} \kappa_2 \left\langle V \left\langle \frac{(n\mathcal{M}_2)' \mathcal{F}_2}{1 + 4\mathcal{F}_2^2} E_{xx} \right\rangle_1 \right\rangle_1,
\end{aligned}$$

where the space and time scale are  $x_0 = \varepsilon F_M l / (eN_D)$  and  $t_0 = x_0 / v_M$  respectively, and we have used  $E = F/F_M$ ,  $J_0 = ev_M N_D / l$ , with

$$\begin{aligned}
\mathcal{F}_2 &= \frac{\langle F \rangle_2}{F_M}, \quad G = \frac{1 - (1 + 2\tau_e^2)\mathcal{F}^2}{(1 + \mathcal{F}^2)^3}, \quad \kappa_1 = \frac{2}{t_0(\nu_{\text{en}} + \nu_{\text{imp}})}, \\
\kappa_2 &= \frac{\Delta l \tau_e}{\hbar x_0 (\nu_{\text{en}} + \nu_{\text{imp}})}, \quad \kappa_3 = \frac{2v_M(1 + \tau_e^2)}{x_0(\nu_{\text{en}} + \nu_{\text{imp}})}, \quad \kappa_4 = \frac{\Delta^2 l^2}{8\hbar^2 v_M (\nu_{\text{en}} + \nu_{\text{imp}}) x_0}.
\end{aligned}$$

The boundary conditions for the QDDE (10), which contains triple spatial averages, need to be specified for the intervals  $[-2l/x_0, 0]$  and  $[Nl/x_0, (Nl + 2l)/x_0]$ , and not just at the points  $x = 0$  and  $x = Nl/x_0$  ( $N$  denotes the number of SL periods spanning the device), as in the case of the parabolic semiclassical GDDE. Similarly, the initial condition has to be defined on the extended interval  $[-2l/x_0, (Nl + 2l)/x_0]$ . Note that the spatial averages in the nonlocal QDDE give rise to finite differences of partial derivatives in the diffusion terms, and therefore lead to a type of equations for which little seems to be known, especially from the numerical point of view.

### 3 Numerical solution of the nonlocal QDDE

The QDDE (10) must be solved together with the voltage bias condition

$$\int_0^L E(x, t) dx = \phi L \quad (11)$$

for the dimensionless electric field  $E$  and total current density  $J$ . Here  $L = Nl/x_0$  is the length of the SL and  $\phi = \Phi/(F_M Nl)$  the dimensionless applied voltage. We have used a constant initial condition  $E(x, t=0) = \phi$ . As boundary conditions in the intervals  $[-2l/x_0, 0]$  and  $[L, L + 2l/x_0]$ , we adopt

$$J - \frac{\partial E}{\partial t} = \frac{\sigma}{\sigma_0} E \quad (12)$$

at all points  $[-2l/x_0, 0]$  of the Ohmic injecting contact, with  $\sigma_0 = e\Delta/(\hbar F_M x_0^2)$ , and zero-flux boundary conditions at the receiving contact  $[L, L + 2l/x_0]$ .

The contact conductivity  $\sigma$  is selected so that  $eN_D v_M V(F/F_M)$  and  $\sigma F$  intersect on the second branch of  $V(\mathcal{F})$ , in which  $dV/d\mathcal{F} < 0$ . This is a typical boundary condition yielding self-sustained oscillations in drift-diffusion SL models [1, 3, 4], from which we have extracted a useful previous knowledge.

#### 3.1 Numerical scheme

The numerical scheme we have used is an efficient implicit scheme for partial differential equations with an integral constraint, described and proved to converge in Ref. [10]. Spatial derivatives are approximated by central differences and a first-order implicit Euler method is used to integrate the resulting differential equations in time. This procedure results in having to solve a system of  $N + 2$  linear equations composed by  $N + 1$  equations for the values of the electric field  $\mathbf{E} = (E_0, \dots, E_N)$  and  $J$  at time  $t^{n+1}$  in terms of their previous values, and the equation for the simple Simpson's rule for the bias condition:

$$T_{i,1}E_{i-1}^{n+1} + T_{i,2}E_i^{n+1} + T_{i,3}E_{i+1}^{n+1} + v_i J^{n+1} = s_i, \quad i = 0, \dots, N, \quad (13)$$

$$E_0^{n+1} + 4E_1^{n+1} + 2E_2^{n+1} + \dots + 2E_{N-2}^{n+1} + 4E_{N-1}^{n+1} + E_N^{n+1} = c. \quad (14)$$

Here  $c = 3\phi/\Delta t$ ,  $\mathbf{T}$  is a tridiagonal matrix, and  $\mathbf{v}$  and  $\mathbf{s}$  are  $(N + 1) \times 1$  column vectors. They contain the nonlinear coefficients of  $E_i$  and  $J$  and the right-hand-side (RHS) of the Euler method respectively, evaluated at time  $t^n$ . Denoting by  $\mathbf{u} = (1, 4, 2, \dots, 2, 4, 1)$  the  $1 \times (N + 1)$  row vector of Simpson's rule, the block matrix formulation of this system is  $\mathbf{T} \cdot \mathbf{E} + J\mathbf{v} = \mathbf{s}$  and  $\mathbf{u} \cdot \mathbf{E} = c$ , which can be efficiently solved by solving the following two systems with the same tridiagonal matrix:

$$\mathbf{T} \cdot \mathbf{y} = \mathbf{s}, \quad \mathbf{T} \cdot \mathbf{z} = \mathbf{v}. \quad (15)$$

In terms of  $\mathbf{y}$  and  $\mathbf{z}$ , we obtain

$$J = \frac{\mathbf{u} \cdot \mathbf{y} - c}{\mathbf{u} \cdot \mathbf{z}}, \quad \mathbf{E} = \mathbf{y} - J\mathbf{z}. \quad (16)$$

Thus we first obtain the  $LU$  factorization of  $\mathbf{T}$  and then we carry out two backsubstitution processes to solve (15). Then (16) yield  $J$  and  $\mathbf{E}$ .

The essential property of the numerical scheme is that  $\mathbf{T}$  is a tridiagonal matrix. To preserve this property, our idea is to write the QDDE (10) in the form of Eq. (13). Thus, we need to extract the coefficients of  $E_{i-1}^{n+1}$ ,  $E_i^{n+1}$ ,  $E_{i+1}^{n+1}$  and  $J^{n+1}$ . The QDDE can be written in the following form:

$$E_t + \langle a(1 + E_x) \rangle_1 - D(E_{xx}) - bJ = \langle B(E_x) \rangle_1, \quad (17)$$

where

$$\begin{aligned} B &= 4\kappa_2 \alpha \langle c_1 \langle E_x \rangle_2 \rangle_1 + \frac{1}{2} \kappa_2 V \langle c_2 \langle E_x \rangle_2 \rangle_1 - \kappa_3 c_3 \langle c_4 \langle E_x \rangle_1 \rangle_1, \\ D &= \kappa_4 \langle \alpha \langle E_{xx} \rangle_1 \rangle_1 - \frac{1}{2} \kappa_1 (1 + \tau_e^2) \left\langle c_3 \left\langle c_5 E_{xx} \right\rangle_1 \right\rangle_1 \\ &\quad - \frac{\kappa_2}{2} \langle \alpha \langle c_6 E_{xx} \rangle_1 \rangle_1 + \frac{\kappa_2}{2} \langle V \langle c_7 E_{xx} \rangle_1 \rangle_1, \\ a &= \mathcal{M} (V + \kappa_1 G \langle \langle n\mathcal{M}V \rangle_1 \rangle_1), \quad b = 1 + \kappa_1 \langle n\mathcal{M}G \rangle_1, \quad \alpha = \frac{1}{1 + \mathcal{F}^2}, \\ c_1 &= \frac{n\mathcal{M}_2 \mathcal{F}_2}{(1 + 4\mathcal{F}_2^2)^2}, \quad c_2 = \frac{n\mathcal{M}_2(1 - 4\mathcal{F}_2^2)}{(1 + 4\mathcal{F}_2^2)^2}, \quad c_3 = \alpha (n\mathcal{M})' V, \\ c_4 &= \frac{n\mathcal{M}(1 - \mathcal{F}^2)}{(1 + \mathcal{F}^2)^2}, \quad c_5 = c_3/\alpha, \quad c_6 = \frac{(n\mathcal{M}_2)'}{1 + 4\mathcal{F}_2^2}, \quad c_7 = c_6 \mathcal{F}_2. \end{aligned}$$

Then we make use of the following two observations:

• **Drift terms:** When we solved the GDDE, we were able to write it in the same form of Eq. (17). Then we observed that the equivalent contribution of  $\langle a(1 + E_x) \rangle_1$  is much greater than the contribution of  $\langle B(E_x) \rangle_1$ , showing that a simple explicit evaluation of this second term in the RHS of Eq. (17) is a good enough approximation. However, the first term must be splitted into

$$\langle a_i(E_i^{n+1})_x \rangle_1 = \frac{1}{6} [a_{i-r}(E_{i-r}^n)_x + 4a_i(E_i^{n+1})_x + a_{i+r}(E_{i+r}^n)_x] \quad (18)$$

$$= \frac{a_i}{3h} E_{i+1}^{n+1} - \frac{a_i}{3h} E_{i-1}^{n+1} + \frac{1}{6} [a_{i-r}(E_{i-r}^n)_x + a_{i+r}(E_{i+r}^n)_x]. \quad (19)$$

Then the first term in (19) must be added to  $T_{3,i}$ , the second to  $T_{1,i}$ , and the third term must go to the RHS.

• **Diffusion terms:** It is computationally more effective to extract from  $D(E_{xx})$  the terms  $d_i$  which contribute to the matrix  $\mathbf{T}$  and then subtracting them from each side of the equation, evaluating  $E_{xx}$  at time  $t^{n+1}$  in the left hand side (implicitly) and at time  $t^n$  in the RHS (explicitly):

$$(E_i^{n+1})_t + \langle a_i(E_i^{n+1})_x \rangle_1 - d_i(E_i^{n+1})_{xx} - b_i J^{n+1} = \langle a_i \rangle_1 + \langle B_i^n \rangle_1 + D_i^n - d_i(E_i^n)_{xx}. \quad (20)$$

From this point of view,  $d_i(E_i^{n+1})_{xx}$  is an approximation of the contribution of the diffusion to the implicit part of the algorithm, and  $D_i^n - d_i(E_i^n)_{xx}$  is a low cost estimation of the rest of the diffusion effects. After some calculations, we obtain  $d_i = d_i(1) + d_i(2) + d_i(3) + d_i(4)$ , where

$$d_i(1) = \frac{\kappa_4}{36} [\alpha_{i-r} + 16\alpha_i + \alpha_{i+r}], \quad (21)$$

$$d_i(2) = -\frac{\kappa_1}{72} (1 + \tau_e^2) [c_{3,i-r} + 16c_{3,i} + c_{3,i+r}] c_{5,i}, \quad (22)$$

$$d_i(3) = -\frac{\kappa_2}{72} [\alpha_{i-r} + 16\alpha_i + \alpha_{i+r}] c_{6,i}, \quad (23)$$

$$d_i(4) = \frac{\kappa_2}{72} [V_{i-r} + 16V_i + V_{i+r}] c_{7,i}. \quad (24)$$

The numerical system can be written finally in the form of Eq. (13) with

$$T_{1,i} = -2k(d_i + \frac{h}{3}a_i), \quad T_{2,i} = 2(h^2 + 2kd_i), \quad T_{3,i} = -2k(d_i - \frac{h}{3}a_i), \quad (25)$$

$$v_i = -2kh^2(1 + \kappa_1 b_i), \quad s_i^n = 2h^2 \left\{ E_i^n + k [D_i^n - d_i(E_i^n)_{xx}] \right\} \quad (26)$$

$$- 2kh^2 \left\{ \frac{1}{6} [a_{i-r}(E_{i-r}^n)_x + a_{i+r}(E_{i+r}^n)_x] + \langle a_i - B_i^n \rangle_1 \right\}, \quad (27)$$

where  $h = \Delta x$  and the equations have been scaled by a factor  $2kh^2$ .

To calculate these coefficients at each time step, we observe that

$$\mathcal{I}_m(\tilde{\mu}) = \frac{1}{\rho_0} \int_{-\pi}^{\pi} \cos(mk) \hat{f}^{\text{FD}}(k, \tilde{\mu}) dk, \quad (28)$$

where  $\rho_0 = m^* k_B T / (\pi \hbar^2 N_D)$  and  $\hat{f}^{\text{FD}} = f^{\text{FD}} / N_D$ . For  $m = 0$ , using expression (3) gives  $\mathcal{I}_0(\tilde{\mu}) = 2\pi n / (\rho_0 N_D)$ , so  $\mathcal{I}_0(M) = 2\pi / \rho_0$ , and then

$$\mathcal{M} \left( \frac{n}{N_D} \right) = \frac{N_D}{n} \frac{\mathcal{I}_1(\tilde{\mu})}{\mathcal{I}_1(M)}, \quad \mathcal{M}_2 \left( \frac{n}{N_D} \right) = \frac{N_D}{n} \frac{\mathcal{I}_2(\tilde{\mu})}{\mathcal{I}_1(M)}. \quad (29)$$

The integrals  $\mathcal{I}_1(M)$  and  $\mathcal{I}_{1,2}(\tilde{\mu})$  are calculated with the Simpson's rule, and the derivatives of  $n\mathcal{M}$  and  $n\mathcal{M}_2$  with respect to  $n$  are estimated numerically.

To do that, we first need to obtain the value of  $\tilde{\mu}$  for a given value of  $n$ , by using (3) and (4). This must be done at each time step for each point of the space discretization (the value of  $M = \tilde{\mu}(n/N_D)$  is obtained only once), and it is one of the bottlenecks of the algorithm. We have used a Newton-Raphson iterative method, which uses the extended Simpson's rule to calculate  $n(\tilde{\mu})$  and  $dn(\tilde{\mu})/d\tilde{\mu}$ , the later using the analytical expression of  $d\hat{f}^{\text{FD}}/d\tilde{\mu}$ . The initial guess for Newton iterations is estimated by averaging the value of  $\tilde{\mu}$  in the previous time step with the following upper and lower bounds of  $\tilde{\mu}$ :

$$\ln(e^{n/(\rho_0 N_D)}) < \tilde{\mu} < \ln(e^{n/(\rho_0 N_D)} - 1) + \delta. \quad (30)$$

When  $n$  is large,  $\tilde{\mu}$  is also large because  $f^{\text{FD}}$  is a monotonically increasing function of  $\mu$  and the linear estimation  $n(\tilde{\mu}) = \rho_0 N_D(\tilde{\mu} - \delta)$  can be used:

$$\tilde{\mu} = \frac{n}{\rho_0 N_D} + \delta. \quad (31)$$

### 3.2 Results

We have used the parameter values of all the superlattices reported in the experimental references [6, 7, 8] with the same satisfactory result. Here we present first a typical case of self-sustained current oscillations accompanied by the motion and recycling of an electric field dipole wave, corresponding to a 157-period 3.64 nm GaAs/0.93 nm AlAs SL [6] at 14K, with  $\Delta = 72$  meV,  $N_D = 4.57 \times 10^{10} \text{cm}^{-2}$ ,  $\nu_{\text{imp}} = 2\nu_{\text{en}} = 18 \times 10^{12}$  Hz under different values of the dimensionless dc voltage bias  $\phi$ . Cathode and anode contact conductivities are 2.5 and  $0.62 \Omega^{-1} \text{cm}^{-1}$ , respectively, and the effective mass is  $m^* = (0.067d_W + 0.15d_B)m_0/l$ , where  $m_0 = 9.109534 \times 10^{-31} \text{Kg}$  is the electron rest mass.

Our numerical solution shows that the current and the field profile become stationary for  $\phi < 0.75$  (1.2 V). For larger values of the dimensionless voltage bias  $\phi$ , the initial field profile evolves toward a stable time-periodic solution for which  $J$  oscillates with time and the field profile shows recycling and motion of a pulse from  $x = 0$  to the SL end.

Fig. 1 shows the self-oscillations of the current for 1.62 V ( $\phi = 1$ ) and the corresponding field pulse at different times. In this figure, we compare the solution of the GDDE corresponding to the semiclassical BGK-Poisson kinetic equation and the solution of the QDDE for  $\Gamma = 18$  meV, which is of the same order as the collision frequencies. Self-oscillations frequency is also an important magnitude to measure; in the QDDE the frequency is  $\nu_Q = 25.5$  Ghz, faster than in the GDDE,  $\nu_G = 20.6$  Ghz (relative frequency  $(\nu_Q - \nu_G)/\nu_G = 23.8\%$ ).

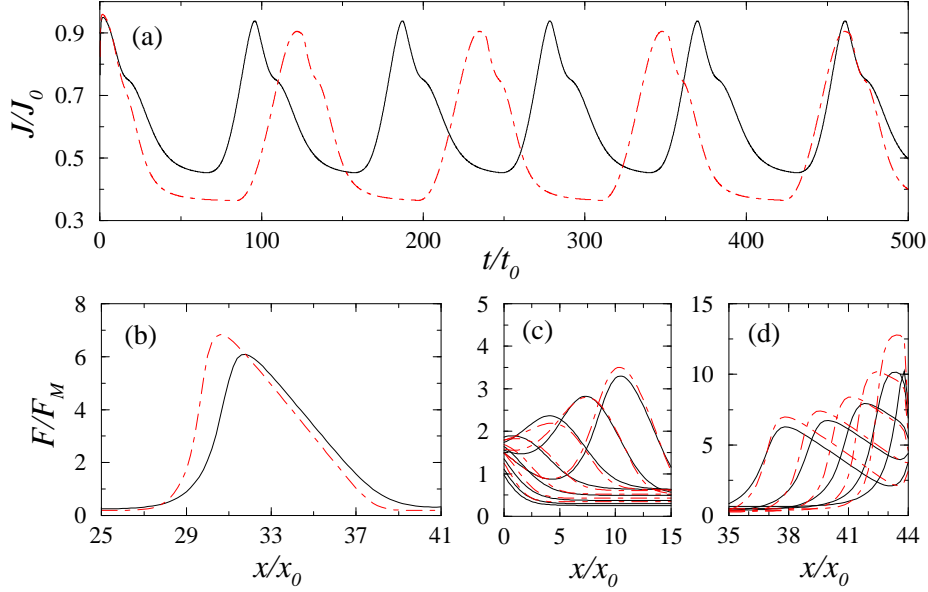


Figure 1: (a) Current ( $J_0 = ev_M N_D/l$ ) vs. time ( $t_0 = \varepsilon F_M/J_0$ ) during self-oscillations for a voltage biased GaAs/AlAs SL, as described by the QDDE (solid line) and by the GDDE (dot-dashed line). (b) Comparison between the fully developed dipole wave for the QDDE (solid line) and the dipole wave for the GDDE (dashed line). (c) Dipole wave at different times during the stage in which it is shed from the injecting contact. (d) Same as (c) for the stage in which the dipole disappears at the anode, located at  $L \approx 44$ . Parameter values are  $x_0 = v_M t_0 = 16$  nm,  $t_0 = 0.43$  ps,  $J_0 = 6.07 \times 10^5$  A/cm<sup>2</sup>,  $\phi = 1$ .

Collision broadening shortens the period of the current oscillations and therefore it reinforces the effects of the nonlocal terms in the QDDE due to quantum effects. See Ref. [5] for details.

The second case we want to show is the *upside-down* case. When we were doing the comparison between the QDDE and the GDDE for all the available experimental data [6, 7, 8], we found a peculiar SL with a large value of the miniband width  $\Delta$  for which the GDDE yields a surprising result: the wave of the electric field appeared reversed and travelling in the opposite direction, and the pulses of the current oscillations were downwards. Fig. 2(B) shows the electric field distribution for this case, corresponding to the current density reversed oscillations shown in Fig. 3.

We are still trying to identify the features of the equation which are responsible of this behavior; the reason seems to be in the fact that the velocity

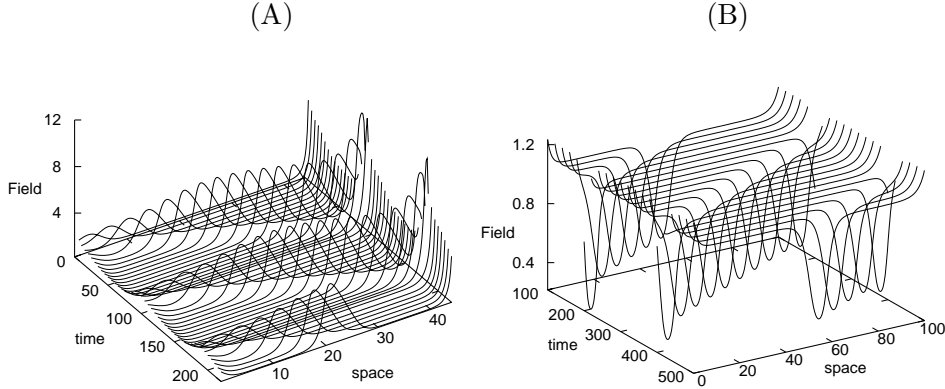


Figure 2: Electric field wave during self-oscillations corresponding to two different experimental situations: (A) the SL used in Fig. 1, as described by the QDDE, and (B) a 130-period 4 nm GaAs/0.6 nm AlAs SL with  $\Delta = 120$  meV,  $N_D = 4.14 \times 10^{10}$  cm $^{-2}$ ,  $\nu_{\text{imp}} = 10^{13}$  Hz  $\nu_{\text{en}} = 0.51 \times 10^{13}$  Hz and the same conductivity  $2.5 \Omega^{-1} \text{cm}^{-1}$  at both contacts, under a dc voltage bias of  $\phi = 1$ .

curve exhibits two local maxima (instead of one) for certain values of the parameters during the simulation; see Fig. 3(B).

In conclusion, we have presented an effective numerical algorithm for a nonlocal quantum drift-diffusion equation based upon prior physical knowledge, taking care of technical details to help the reader in the reproduction of our results.

## Acknowledgments

This work has been supported by the MCyT grant BFM2002-04127-C02-01, and by the European Union under grant HPRN-CT-2002-00282. R. Escobedo has been supported by a postdoctoral grant awarded by the Consejería de Educación of the Autonomous Region of Madrid.

## References

- [1] L. L. BONILLA, “Theory of Nonlinear Charge Transport, Wave Propagation and Self-oscillations in Semiconductor Superlattices”, *J. Phys.: Condens. Matter* **14** (2002) R341–R381.

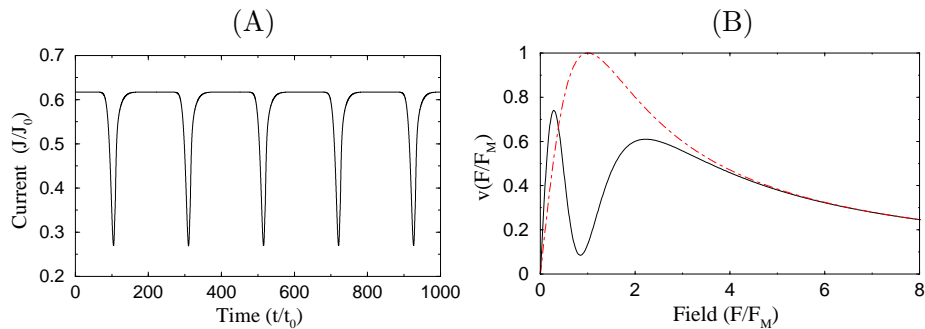


Figure 3: (A) Downwards pulses of the current during self-oscillations for the second SL used in this paper, and (B) possible explanation of this surprising and probably unrealistic feature: during the simulation, the velocity exhibits two maxima (solid line). Dashed line is the typical phenomenological drift velocity used in drift-diffusion models.

- [2] P. L. BHATNAGAR, E. P. GROSS, AND M. KROOK, “A Model for Collision Processes in Gases. I. Small Amplitude Processes in Charged and Neutral One-Component Systems”, *Phys. Rev.* **94** (1954) 511–525.
- [3] L.L. BONILLA, R. ESCOBEDO AND A. PERALES, “Generalized drift-diffusion model for miniband superlattices”, *Phys. Rev. B* **68** (2003) 241304 (4 pages).
- [4] A. PERALES, L.L. BONILLA, R. ESCOBEDO, “Miniband transport and oscillations in semiconductor superlattices”, *Nanotechnology* **15** (2004) S229–S233.
- [5] L. L. BONILLA, R. ESCOBEDO, “Wigner-Poisson and nonlocal drift-diffusion model equations for semiconductor superlattices”, *Math. Mod. Meth, in Appl. Sci.* to appear (2005) 1–19.
- [6] E. SCHOMBURG, T. BLOMEIER, K. HOFBECK, J. GRENZER, S. BRANDL, I. LINGOTT, A. A. IGNATOV, K. F. RENK, D. G. PAVELEV, Y. KOSCHURINOV, B. Y. MELZER, V.M. USTINOV, S. V. IVANOV, A. ZHUKOV, AND P. S. KOPEV, “Current oscillations in superlattices with different miniband widths”, *Phys. Rev. B* **58** (1998) 4035–4038.
- [7] R. SCHEUERER, E. SCHOMBURG, K. F. RENK, “Feasibility of a semiconductor superlattice oscillator based on quenched domains for the generation of submillimeter waves”, *Appl. Phys. Lett* **81**, (2002) 1515–1517.

- [8] E. SCHOMBURG ET AL., “ $\Delta = 120meV...$  to be filled in final version”, ,  
( ) –.
- [9] A. A. IGNATOV AND V.I. SHASHKIN, “Bloch oscillations of electrons and instability of space-charge waves in semiconductor superlattices”, *Sov. Phys. JETP* **66** (1987) 526–530.
- [10] A. CARPIO, P.J. HERNANDO AND M. KINDELAN, “Numerical study of hyperbolic equations with integral constraints arising in semiconductor theory”, *SIAM J. Numer. Anal.* **39** (2001) 168–191